Elastic-Plastic Fracture of Circumferential Through-Wall Cracked Pipe Welds Subject to Bending

S. Rahman

F. Brust

Engineering Mechanics Department,
Battelle,
Columbus, OH 43201

A methodology is proposed to carry out elastic-plastic fracture analysis of through-wall cracked ductile pipe weldments subjected to pure bending loads. It is based on deformation theory of plasticity, constitutive law characterized by Ramberg-Osgood model, and an equivalence criteria incorporating reduced thickness analogy for simulating system compliance due to the presence of a crack in weld metal. Closed-form solutions are obtained in terms of elementary functions for approximate evaluation of energy release rate and center crack opening displacement. The method utilizes material properties of both base and weld metals which are not considered in the current estimation methods. It is general and can be applied in the complete range between elastic and fully plastic conditions. Numerical examples are presented to illustrate the proposed technique. Comparisons of results with reference solutions from finite element method indicate satisfactory prediction of foregoing fracture parameters.

1 Introduction

The evaluation of energy release rates (also known as J-integral) and center crack opening displacements (COD) of circumferentially located through-wall cracked (TWC) pipe weldments is an important issue in the structural integrity assessment of leak-before-break and in-service flaw acceptance criteria for nuclear piping. Recent analytical, experimental, and computational studies on this subject indicate that the J and COD are the most viable fracture parameters for characterizing crack initiation, stable crack growth, and the subsequent instability in ductile materials (Rice, 1968; Hutchinson, 1982; Kanninen and Popelar, 1985). They are usually determined by numerical analysis and estimation techniques. Traditionally, a comprehensive numerical study has been based on sophisticated finite element method (FEM) for nonlinear stress analysis. Although several general and special-purpose computer codes are currently available for FEM, the inconvenience with regard to its applicability as a practical analysis tool is not of minor nature. The computational effort is still significant, even with the recent development of numerical techniques and industry-standard computational facilities. In addition, the employment of FEM can be time-consuming and may require a high degree of expertise for its implementation. These issues become particularly significant when numerous deterministic analyses are required in a full probabilistic analysis.

Contributed by the Pressure Vessels and Piping Division and presented at the Pressure Vessels and Piping Conference, San Diego, California, June 23-27, 1991, of THE AMERICAN SOCIETY OF MECHANICAL ENGINEERS. Manuscript received by the PVP Division, April 30, 1992; revised manuscript received July 28, 1992. Associate Technical Editor: Y. Asada.

Currently, there are several simplified methods available for elastic-plastic fracture analysis of piping systems. They were primarily developed for flawed pipes with cracks in base metal. No reliable estimation techniques exist to evaluate performance of pipes with cracks in weld metal (Rahman et al., 1991). The energy release rate and crack opening displacement for pipe weldment cases are typically estimated assuming that the entire pipe is made up of all base material. Predictions are usually made using base metal stress-strain data and weld metal J-resistance curve (Wilkowski et al., 1989). This can lead to overly conservative or nonconservative predictions, depending on the strength ratio of the base versus weld material.

In this paper, a methodology is developed to predict the J-integral and COD of TWC ductile pipe weldments subjected to remote bending loads. It is based on (*i*) classical deformation theory of plasticity, (*ii*) constitutive law characterized by Ramberg-Osgood model, and (*iii*) an equivalence criteria incorporating reduced thickness analogy for simulating system compliance due to the presence of a crack in weld metal (Rahman et al., 1991). The method utilizes material properties of both base and weld metals. The method is general in the sense that it may be applied in the complete range between elastic and fully plastic conditions. Since it is based on J-tearing theory, it is subject to the usual limitations imposed upon this theory, e.g., proportional loading, etc. This implies that the crack growth must be small, although in practice J-tearing methodology is used far beyond the limits of its theoretical validity with acceptable results (Wilkowski et al., 1989). Numerical examples are presented to illustrate the proposed technique which is verified with the results from FEM.

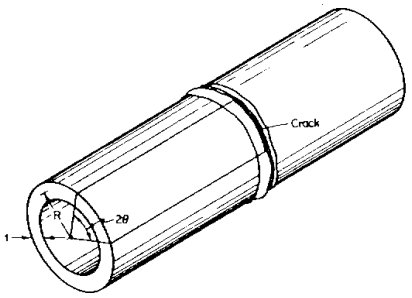

Fig. 1 Circumferential crack in a pipe butt weld

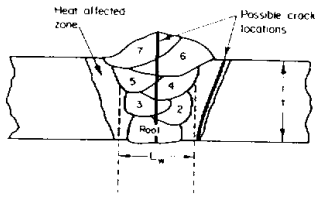

Fig. 2 Typical butt-weld sequence for a pipe and possible cracks (this is an actual sequence for a 4-in-dia schedule 80 pipe)

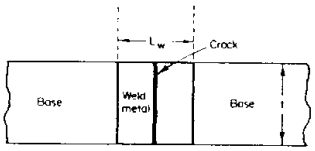

Fig. 3 Idealized pipe weld with a crack

2 Pipe Weld With a Single Crack

Consider Fig. 1 which illustrates a typical butt-welded pipe with a circumferential through-wall crack of total angle 2θ. The pipe mean radius R and thickness t are shown. Figure 2 illustrates the typical geometry for a butt weld in a pipe. Typically, the weld layers are deposited in sequence. The example of Fig. 2 is an actual sequence from a 4-in-(102-mm-) dia schedule 80 pipe, which required seven passes. The welding gives rise to a heat-affected zone (HAZ), which results in material properties different from those in the weld metal or base metal alone. Often cracks develop in the HAZ zones of pipe and may grow in a skewed fashion to become a through-wall crack as illustrated in that figure. Figure 2 also shows a crack which grows through the weld metal, and this is the type of crack assumed in the development of the method presented here. Figure 3 shows the pipe weld geometric assumption made here. Note that the angular and irregular nature of the actual weldment is assumed to be a straight radial bimaterial interface line for development of this model. Residual stresses and altered HAZ properties are not included. The total length of the weldment is assumed to be an average length (Figs 2 and 3), L_w, which is often best approximated to be the pipe thickness.

3 General Background

Consider a simply supported TWC pipe under remote bending moment M in Fig. 4, which has length L, mean radius R, thickness t, and crack angle 2θ with the crack circumferentially located in the weld material of length L_w. In the development of a J-estimation scheme, it is generally assumed that the load point rotation due to the presence of crack ϕ^c, energy release rate J, and center crack opening displacement δ, admit additive decomposition of elastic and plastic components

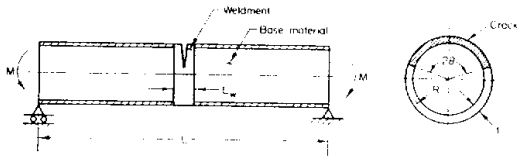

Fig. 4 Schematics of pipe weldments with a circumferential flaw

$$\phi^c = \phi_e^c + \phi_p^c \tag{1}$$

$$J = J_e + J_p \tag{2}$$

$$\delta = \delta_e + \delta_p \tag{3}$$

where the subscripts e and p refer to elastic and plastic contributions. In the elastic range, ϕ_e^c and M are uniquely related. In addition, if the deformation theory of plasticity holds, a unique relationship also exists between ϕ_p^c and M. Once these relationships are determined, the elastic and the plastic components of J and δ can be obtained readily.

4 Energy Release Rate

4.1 Elastic Solution. The elastic energy release rate J_e can be defined as

$$J_e = \frac{\partial U^T}{\partial A} = \frac{\partial}{\partial A}\,(U^c + U^{nc}) = \frac{\partial U^c}{\partial A} \tag{4}$$

where U^T is the total internal strain energy, U^{nc} is the strain energy which would exist if there were no crack present, $U^c = U^T - U^{nc}$ is the additional strain energy in the pipe due to the presence of crack, and $A = 2R\theta t$ is the crack area. When $t \to 0$, i.e., for thin-walled pipe with mode-I crack growth, J_e can be obtained as

$$J_e = \frac{K_I^2}{E} \tag{5}$$

where E is the common elastic modulus of both base and weld materials, and K_I is the mode-I stress intensity factor. From theory of linear elastic fracture mechanics, K_I is given by

$$K_I = \sigma\sqrt{\pi R\theta}\; F_B(\theta) \tag{6}$$

in which $\sigma = M/\pi R^2 t$ is the far-field applied stress, and $F_B(\theta)$ is a geometry function relating K_I of a cracked shell to that for the same size of crack in an infinite plate. From Eqs. (4)–(6), U^c can be integrated to yield

$$U^c = \frac{M^2}{2\pi R^2 tE}\, I_B(\theta) \tag{7}$$

where

$$I_B(\theta) = 4\int_0^\theta \xi F_B(\xi)^2 d\xi \tag{8}$$

Using Castigliano's theorem

$$\phi_e^c = \frac{\partial U^c}{\partial M} \tag{9}$$

which, when combined with Eq. (7), gives

$$M = \frac{E\pi R^2 t}{I_B(\theta)}\,\phi_e^c \tag{10}$$

representing relationship between moment and elastic rotation. Equations (5) and (6) completely specify the elastic energy release rate J_e, and hence the elastic solution is complete in a closed form. Equation (10) provides relationship between ap-

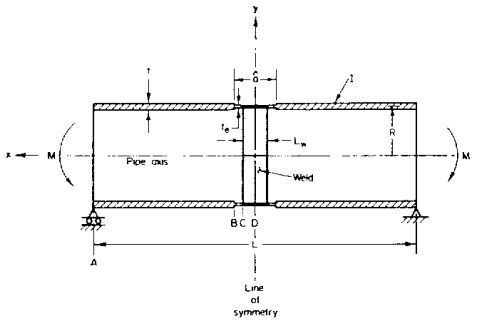

Fig. 5 Reduced section analogy

plied moment M and elastic rotation ϕ_e^c, which will be required for the calculation of J_p explained in the next section. These developments are based on elastic solutions by Sanders (1982, 1983). Explicit functional forms of $F_B(\theta)$ and $I_B(\theta)$ are provided in Appendix A.

4.2 Plastic Solution. The plastic energy release rate J_p can be defined as

$$J_p = -\int_0^{\phi_p^c} \frac{\partial M}{\partial A}\bigg|_{\xi} d\xi \tag{11}$$

where ξ is a dummy variable representing instantaneous plastic rotation. The evaluation of J_p in Eq. (11) requires determination of $M - \phi_p^c$ (or $M - \xi$) relationship as a function of crack size. When this relationship is obtained, Eq. (11) can be used to find J_p and then can be added to J_e to determine the total J.

A widely used univariate constitutive law describing material's stress-strain ($\sigma - \epsilon$) relation is the normalized Ramberg-Osgood model given by

$$\frac{\epsilon}{\epsilon_{0i}} = \frac{\sigma}{\sigma_{0i}} + \alpha_i \left(\frac{\sigma}{\sigma_{0i}}\right)^{n_i} \tag{12}$$

where σ_{0i} is some reference stress usually assumed to be the yield stress, $\epsilon_{0i} = \sigma_{0i}/E$ is the associated reference strain, α_i, n_i are the power-law parameters of model usually chosen to fit experimental data, and $i = 1$ or 2 representing base or weld materials, respectively. In applying the Ramberg-Osgood relation to the cracked pipe problem, it is necessary to relate the stresses with rotations. Ilyushin (1946) showed that the field solutions to the boundary value problem involving a monotonically increasing load or displacement-type parameter is "proportional." Consequently, Eq. (12) applies (minus the elastic term) and the deformation theory plasticity is assumed to be valid. Thus, it can be shown that (Brust and Gilles, 1990; Brust, 1987; Gilles and Brust, 1989)

$$\phi_p^c = L_B^c \alpha_i \left(\frac{\sigma}{\sigma_{0i}}\right)^{n_i - 1} \phi_e^c \tag{13}$$

in which the moment-elastic rotation relationship in Eq. (10) is utilized. In Eq. (13), L_B^c is an unknown function which needs to be determined. For the crack problem, L_B^c may be determined via numerical method. However, no analytical method exists to obtain L_B^c in closed form. Thus, the main task in this methodology is to establish L_B^c in Eq. (13).

Evaluation of L_B^c. Suppose the actual pipe can be replaced by a pipe with reduced thickness t_e which extends for a distance $\hat{a} \geq L_w$ at the center (Fig. 5). Far from the crack plane, the rotation of the pipe is not greatly influenced by whether a crack exists or some other discontinuity is present, as long as the discontinuity can approximate the effects of crack. The reduced thickness section, which actually results in material discontinuity, is an attempt to simulate the reduced system compliance due to the presence of crack. This equivalence approach was originally suggested by Brust (1987) and successfully implemented to evaluate performance of TWC pipes consisting of one single material under various loading conditions (Brust, 1987; Gilles and Brust, 1989). It is assumed here that the deformation theory of plasticity controls stress-strain response and that the beam theory holds.

Consider the equivalent pipe with material discontinuity in Fig. 5, which is subjected to bending load M at both ends. Using classical beam theory, the ordinary differential equations governing displacement of beams with Ramberg-Osgood constitutive law can be easily derived. These equations, when supplemented by the appropriate boundary and compatibility conditions, can be solved following elementary operations of calculus. Details of algebra associated with these solutions are provided in Appendix B. The rotations—dy/dx in Eqs. (30), (33), and (36)—provide explicit relationships between far-field plastic rotation ϕ_p^d due to material discontinuity and the corresponding elastic rotations ϕ_e^d where the new superscript d refers to material discontinuity. Each of these relationships can be expressed in the form analogous to Eq. (13) as

$$\phi_p^d = L_B^d \alpha_i \left(\frac{\sigma}{\sigma_{0i}}\right)^{n_i - 1} \phi_e^d \tag{14}$$

in which L_B^d will depend on geometry, material properties of base and weld metals, t_e and the spatial coordinate x. While no attempt is made here for a formal proof, it is assumed here that L_B^d determined from discontinuity solution (Eq. (14)) approaches the actual unknown L_B^c in Eq. (13).

Since L_B^d evaluated at segment CD cannot account for base material properties (Eq. (36)), the appropriate choice is to write L_B^d at either segment AB or BC. More specifically, when the spatial location is selected to be the point B (i.e., $x = \hat{a}/2$), the explicit version of Eq. (14) becomes

$$\phi_p^d = \frac{\left(\frac{M}{M_{01}}\right)^{n_1}\left(\frac{\hat{a}}{2} - \frac{L_w}{2}\right)\left(\frac{t}{t_e}\right)^{n_1} + \left(\frac{M}{M_{02}}\right)^{n_2}\frac{L_w}{2}\left(\frac{t}{t_e}\right)^{n_2}}{\left(\frac{M}{M_1^*}\right)\epsilon_{01}\left(\frac{\hat{a}}{2} - \frac{L_w}{2}\right)\frac{t}{t_e} + \left(\frac{M}{M_2^*}\right)\epsilon_{02}\frac{L_w}{2}\frac{t}{t_e}} \phi_e^d \tag{15}$$

where $M_i^* = \sigma_{0i} I/R$ is the elastic bending load corresponding to reference stress σ_{0i}, and other parameters are defined in Appendix B. Equation (15) can be derived from Eq. (33) with the constant C_3 replaced by its expression given in Eq. (40). Comparing Eq. (15) with Eq. (14) gives

$$L_B^d = \frac{\left(\frac{M}{M_{01}}\right)^{n_1}\left(\frac{\hat{a}}{2} - \frac{L_w}{2}\right)\left(\frac{t}{t_e}\right)^{n_1} + \left(\frac{M}{M_{02}}\right)^{n_2}\frac{L_w}{2}\left(\frac{t}{t_e}\right)^{n_2}}{\left(\frac{M}{M_1^*}\right)\epsilon_{01}\left(\frac{\hat{a}}{2} - \frac{L_w}{2}\right)\frac{t}{t_e} + \left(\frac{M}{M_2^*}\right)\epsilon_{02}\frac{L_w}{2}\frac{t}{t_e}} \times \frac{1}{\alpha_1\left(\frac{M}{M_1^*}\right)^{n_1 - 1}} \tag{16}$$

Equation (16) apparently indicates that L_B^d has explicit functional dependency on external load parameter M, thus violating previously invoked Ilyushin's theorem (cf., Eq. (13)). However, it can be shown that for the variation of load magnitude in the practical range, the correlation between L_B^d and M is not of strong nature. This is semi-empirically proved by Rahman and Brust (1991).

Determination of t_e. The equivalent reduced thickness t_e can be obtained by forcing the limit moment of reduced pipe section

$$M_L^d = 4\sigma_{\text{limit}} R^2 t_e \tag{17}$$

to be equivalent to the limit moment of cracked pipe section

$$M_L^c = 4\sigma_{\text{limit}} R^2 t \left(\cos\frac{\theta}{2} - \frac{1}{2}\sin\theta\right) \tag{18}$$

giving (Brust, 1987)

$$t_e = t\left(\cos\frac{\theta}{2} - \frac{1}{2}\sin\theta\right) \tag{19}$$

which does not require any explicit description of the limit stress σ_{limit} due to its cancellation in the equality of Eqs. (17) and (18). However, Brust (1987) has observed that Eq. (19) provides fairly good approximation only for small crack angles ($0 \text{ deg} \le 2\theta \le 90 \text{ deg}$). For large crack angles ($2\theta \ge 120$ deg), t_e is found to be better represented by

$$t_e = \frac{4}{\pi} t\left(\cos\frac{\theta}{2} - \frac{1}{2}\sin\theta\right) \tag{20}$$

obtained when the limit moment of the reduced section pipe is calculated from linear stress variation with maximum stress σ_{limit} (giving $M_L^d = \pi\sigma_{\text{limit}} R^2 t_e$) rather than a uniform stress block, as assumed in Eqs. (17) and (18). For cracks with angles in the intermediate range ($90 \text{ deg} \le 2\theta \le 120$ deg), t_e can be found from linear interpolation between these limits (Brust, 1987).

Estimation of J_p. Having determined L_B^d and t_e, the $M - \phi_p^c$ relationship can be obtained from Eq. (14) via $M - \phi_e^c$ relation in Eq. (10). When it is placed in Eq. (11), it can be integrated out symbolically to evaluate J_p in a closed form. Following simple algebra, it can be shown that

$$J_p = \frac{\alpha_1}{E\sigma_{01}^{n_1-1}} \frac{1}{n_1+1} \frac{\pi R}{2} H_B L_B^d J_B \left(\frac{M}{\pi R^2 t}\right)^{n_1+1} \tag{21}$$

where

$$H_B = \frac{1}{I_B}\frac{\partial I_B}{\partial\theta} + \frac{1}{L_B^d}\frac{\partial L_B^d}{\partial\theta} \tag{22}$$

which involves the partial derivatives $\partial I_B/\partial\theta$ and $\partial L_B^d/\partial\theta$ explicitly described in Appendix C. Equations (5) and (21) provide closed-form expressions for J_e and J_p. These analytic forms are very convenient for both deterministic and probabilistic elastic-plastic fracture mechanics.

5 Center Crack Opening Displacement

5.1 Elastic Solution. The elastic component δ_e may be obtained from any known solution in the literature, such as Sanders' solution (1982, 1983), as interpreted by Yoo and Pan (1988). However, when this closed-form solution based on shell theory is compared with experimental data and the GE/EPRI finite element solutions (1981), the elastic COD appears to be underpredicted. Besides, Paul et al. (1991) show that the GE/EPRI solutions compare well with both test data and separate finite element solutions. Hence, the following GE/EPRI solution given by:

$$\delta_e = 4a\frac{R}{I} V_1\left(\frac{\theta}{\pi}, \frac{R}{t}\right)\frac{M}{E} \tag{23}$$

is used in this paper. In Eq. (23), $a = R\theta$ is the half-crack length, $I = \pi R^3 t$ is the moment of inertia of the uncracked pipe section with large R/t, and V_1 is the crack opening displacement function tabulated by Kumar et al. (1981) for various combinations of θ/π and R/t.

Table 1 Parameters of Ramberg-Osgood model

Material (i)	σ_{0i} (MPa)	E (MPa)	α_i	n_i
Base metal	303.3	175760	30.56	3.826
Weld metal	358.5	175760	11.96	9.370

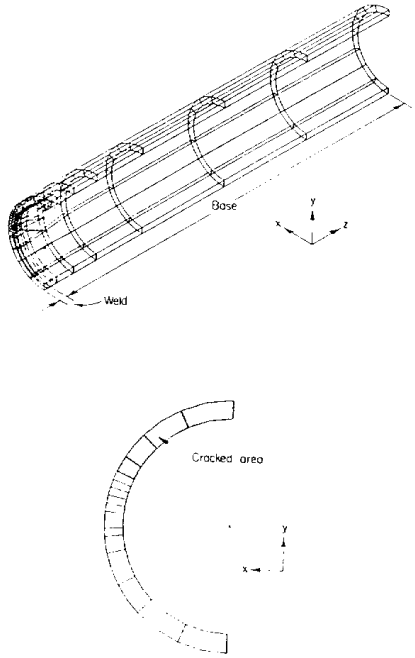

Fig. 6 Finite element mesh of cracked pipe weld

5.2 Plastic Solution. The plastic component δ_p can be obtained from

$$\delta_p = \left[R\left(1 + \sin\frac{\theta}{2}\right)\right]\phi_p^c \tag{24}$$

where ϕ_p^c is the plastic rotation of pipe due to the crack. In Eq. (24), the term $R[1 + \sin(\theta/2)]$ represents the distance from the rigid plastic neutral axis to the center of the crack. Hence, it is clear that the foregoing equation should, at worst, provide a conservative prediction.

6 Numerical Examples

Consider two circumferential TWC pipe weldments, one with $R = 52.87$ mm and $t = 8.56$ mm ($R/t \simeq 6$), and the other with $R = 55.88$ mm and $t = 3.81$ mm ($R/t \simeq 15$), each of which is subjected to constant bending moment M applied at the simply supported ends. In both pipes, it is assumed that $2\theta = 139$ deg and $L_w = 5.59$ mm. The constitutive law for base and weld metals are assumed to follow the Ramberg-Osgood model. The numerical values of reference stress σ_{0i}, modulus of elasticity E, and the model parameters α_i and n_i are shown in Table 1.

The pipes with Table 1 input parameters are used to calculate energy release rates J and crack opening displacement δ by both estimation method and nonlinear finite element method

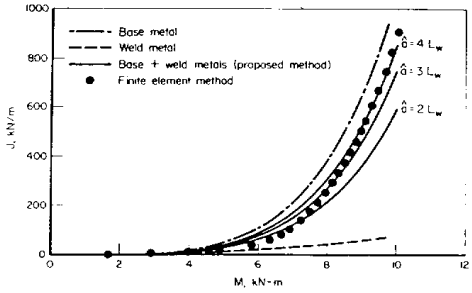

Fig. 7(a) Comparisons of J versus M by various methods (R/t = 6)

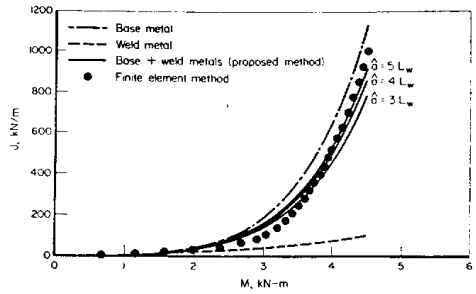

Fig. 8(a) Comparisons of J versus M by various methods (R/t = 15)

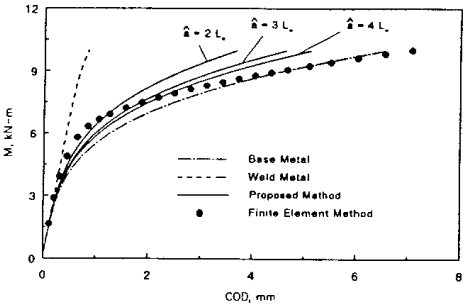

Fig. 7(b) Comparisons of COD versus M by various methods (R/t = 6)

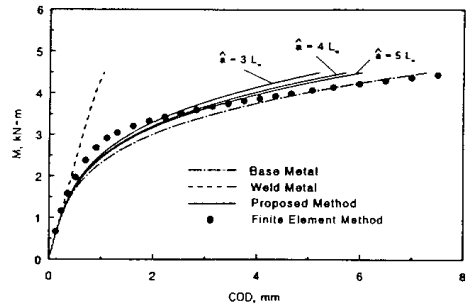

Fig. 8(b) Comparisons of COD versus M by various methods (R/t = 15)

(FEM). Approximate evaluation of J and δ by the proposed estimation scheme is based on Eqs. (2), (5), and (21), and Eqs. (3), (23), and (24), respectively. The FEM solutions, on the other hand, are based on 3-dimensional brick elements available in the fracture mechanics code BCLFEM, which is developed by in-house expertise of the computational group at Battelle. Figure 6 shows a typical mesh representing the finite element idealization of the quarter (due to symmetry) of TWC pipe with crack in weld.

Figures 7 and 8 show several plots of J versus M and δ versus M obtained from various levels of approximation for both pipes with R/t = 6 and R/t = 15. Also shown in these figures are the results of finite element method (FEM), which can be used as benchmark solutions for evaluating the accuracy of the analytical methods. Comparisons of the results of approximate method developed by Brust and Gilles (1990) solely based on all-base or all-weld material properties with those of FEM suggest that they provide only upper and lower bounds of the fracture parameters at any given load M. However, neither of them can be used to predict their actual values reliably.

Figures 7 and 8 also exhibit the results of the proposed method for several values of $\hat{a}$ representing the length of reduced thickness section. They all show reasonably good agreement with the solutions of FEM. Although $\hat{a}$ is treated here as a free parameter, an optimum value $\hat{a}_{opt}$ needs to be determined for obtaining the best estimate. In a recent paper by Rahman and Brust (1991), several finite element analyses are carried out to determine the optimum value of $\hat{a}$. Following extensive comparisons with the results of finite element analysis, the optimum value $\hat{a}_{opt}$ is found to be relatively insensitive to the variations in the hardening parameters n_1 and n_2 of the Ramberg-Osgood models for the base and weld metals, respectively. It is also found that the optimum value of $\hat{a}_{opt}/L_w$ is roughly in the neighborhood of 4 where L_w is the average length of weld metal in the pipe. Details of this calibration procedure can be obtained from Rahman and Brust (1991). The results of this calibration, however, should be viewed as a preliminary estimate of $\hat{a}_{opt}$. More refined calibration will need to be performed to investigate dependency on the geometry factor (e.g., R/t ratio), crack size (e.g., θ/π ratio), reference stress ratio (e.g., σ_{01}/σ_{02}), and any other pertinent parameters.

7 Conclusions

A methodology is proposed to estimate the energy release rate and center crack opening displacement of TWC ductile pipe weldments subjected to remote bending loads. The method is based on deformation theory of plasticity, constitutive law characterized by Ramberg-Osgood model, and an equivalence criteria incorporating reduced thickness analogy for simulating system compliance due to the presence of a crack in weld metal. The method utilizes material properties of both base and weld metals which are not considered in the current estimation methods. The method is general and it can be applied in the complete range between elastic and fully plastic conditions.

Several numerical examples are presented to illustrate the proposed technique for estimating the J-integral and COD of TWC ductile pipe welds. Similar results from stress analysis based on finite element analysis are also obtained to provide reference solutions for the foregoing problems. Comparison of the results predicted by this new method with the finite element analyses indicate satisfactory predictions of energy release rate and crack opening displacement.

The equations for J-integral and COD in a nonlinearly elastic cracked pipe weld are derived in closed form in terms of elementary functions. This makes the proposed scheme computationally feasible and attractive for future development of probabilistic fracture mechanics by both analytical and simulation models.

References

Brust, F. W., 1987, "Approximate Methods for Fracture Analysis of Through-Wall Cracked Pipes," Topical Report, Battelle Columbus Laboratories, NUREG/CR-4853.

Brust, F. W., and Gilles, P., 1990, "An Equivalence Method for Estimating Energy Release Rates With Application to Cracked Cylinders," ASME JOURNAL OF PRESSURE VESSEL TECHNOLOGY, submitted for publication.

Gilles, P., and Brust, F. W., 1989, "Approximate Methods for Fracture Analysis of Tubular Members Subjected to Combined Tensile and Bending Loads," *Proceedings of the 8th International Conference on Offshore Mechanics and Arctic Engineering*, Hague, The Netherlands.

Hutchinson, J. W., 1982, "Fundamentals of the Phenomenological Theory of Nonlinear Fracture Mechanics," ASME *Journal of Applied Mechanics*, Vol. 49, pp. 103-107.

Ilyushin, A. A., 1946, "The Theory of Small Elastic-Plastic Deformations," *Prikadnaia Matematika i Mekhanika*, PMM, Vol. 10, pp. 347-356.

Kanninen, M., and Popelar, C., 1985, *Advanced Fracture Mechanics*, Oxford University Press, Inc., New York, NY.

Kumar, V., German, M., Wilkening, W., Andrews, W., deLorenzi, W., and Mowbray, D., 1984, "Advances in Elastic-Plastic Fracture Analysis," Final Report, EPRI/NP-3607.

Paul, D. D., et al., 1991, "Evaluation of Refinement of Leak-Rate-Estimation Models," Topical Report, Battelle Columbus Laboratories, NUREG/CR-4572.

Rahman, S., and Brust, F., 1991, "An Estimation Method for Evaluating Energy Release Rates of Circumferential Through-Wall Cracked Pipe Welds," *Engineering Fracture Mechanics*, in press.

Rahman, S., Brust, F., Nakagaki, M., and Gilles, P., 1991, "An Approximate Method for Estimating Energy Release Rates of Through-Wall Cracked Pipe Weldments," *Fracture, Fatigue, and Risk*, ASME PVP-Vol. 215, pp. 87-92.

Rice, J. R., 1968, "A Path-Independent Integral and the Approximate Analysis of Strain Concentration by Notches and Cracks," ASME *Journal of Applied Mechanics*, Vol. 35, pp. 376-386.

Sanders, J. L., Jr., 1982, "Circumferential Through-Cracks in Cylindrical Shells Under Tension," ASME *Journal of Applied Mechanics*, Vol. 49, pp. 103-107.

Sanders, J. L., Jr., 1983, "Circumferential Through-Crack in a Cylindrical Shell Under Combined Bending and Tension," ASME *Journal of Applied Mechanics*, Vol. 50, p. 221.

Wilkowski, G. M., et al., 1989, "Degraded Piping Program—Phase II," Final and Semi-Annual Reports (1985-1989), by Battelle Columbus Laboratories, NUREG/CR-4082, Vols. 1-8.

Yoo, S. H., and Pan, J., 1988, "Closed-Form Displacement Solutions for Circumferentially Cracked Pipes in Bending and Tension," University of Michigan Report No. UM-MEAM-88-06.

APPENDIX A

The following are the approximate equations for $F_B(\theta)$ and $I_B(\theta)$ (Brust, 1987):

$$F_B(\theta) = 1 + A_b\left(\frac{\theta}{\pi}\right)^{1.5} + B_b\left(\frac{\theta}{\pi}\right)^{2.5} + C_b\left(\frac{\theta}{\pi}\right)^{3.5} \tag{25}$$

with

$$A_b = -3.2654 + 1.5278\left(\frac{R}{t}\right) - 0.0727\left(\frac{R}{t}\right)^2 + 0.0016\left(\frac{R}{t}\right)^3$$

$$B_b = 11.3632 - 3.9141\left(\frac{R}{t}\right) + 0.1862\left(\frac{R}{t}\right)^2 - 0.0041\left(\frac{R}{t}\right)^3$$

$$C_b = -3.1861 + 3.8476\left(\frac{R}{t}\right) - 0.1830\left(\frac{R}{t}\right)^2 + 0.0040\left(\frac{R}{t}\right)^3 \tag{26}$$

and

$$I_B(\theta) = 2\theta^2\left[1 + 8\left(\frac{\theta}{\pi}\right)^{1.5} I_{b_1} + \left(\frac{\theta}{\pi}\right)^3 (I_{b_2} + I_{b_3})\right] \tag{27}$$

where

$$I_{b_1} = \frac{A_b}{7} + \frac{B_b}{9}\left(\frac{\theta}{\pi}\right) + \frac{C_b}{11}\left(\frac{\theta}{\pi}\right)^2$$

$$I_{b_2} = \frac{A_b^2}{2.5} + \frac{A_b B_b}{1.5}\left(\frac{\theta}{\pi}\right) + \frac{2A_bC_b + B_b^2}{3.5}\left(\frac{\theta}{\pi}\right)^2$$

$$I_{b_3} = \frac{B_bC_b}{2}\left(\frac{\theta}{\pi}\right)^3 + \frac{C_b^2}{4.5}\left(\frac{\theta}{\pi}\right)^4 \tag{28}$$

APPENDIX B

Using classical beam theory for small deformation, the governing differential equations are (Fig. 5):

1 Segment AB ($\hat{a}/2 \le x \le L/2$)

$$\frac{d^2y}{dx^2} = \frac{1}{R}\left(\frac{M}{M_{01}}\right)^{n_1} \tag{29}$$

$$\frac{dy}{dx} = \frac{1}{R}\left(\frac{M}{M_{01}}\right)^{n_1} x + C_1 \tag{30}$$

$$y = \frac{1}{R}\left(\frac{M}{M_{01}}\right)^{n_1} \frac{x^2}{2} + C_1x + C_2 \tag{31}$$

2 Segment BC ($L_w/2 \le x \le \hat{a}/2$)

$$\frac{d^2y}{dx^2} = \frac{1}{R}\left(\frac{M}{M_{01}}\right)^{n_1}\left(\frac{t}{t_e}\right)^{n_1} \tag{32}$$

$$\frac{dy}{dx} = \frac{1}{R}\left(\frac{M}{M_{01}}\right)^{n_1}\left(\frac{t}{t_e}\right)^{n_1} x + C_3 \tag{33}$$

$$y = \frac{1}{R}\left(\frac{M}{M_{01}}\right)^{n_1}\left(\frac{t}{t_e}\right)^{n_1} \frac{x^2}{2} + C_3x + C_4 \tag{34}$$

3 Segment CD ($0 \le x \le L_w/2$)

$$\frac{d^2y}{dx^2} = \frac{1}{R}\left(\frac{M}{M_{02}}\right)^{n_2}\left(\frac{t}{t_e}\right)^{n_2} \tag{35}$$

$$\frac{dy}{dx} = \frac{1}{R}\left(\frac{M}{M_{02}}\right)^{n_2}\left(\frac{t}{t_e}\right)^{n_2} x + C_5 \tag{36}$$

$$y = \frac{1}{R}\left(\frac{M}{M_{02}}\right)^{n_2}\left(\frac{t}{t_e}\right)^{n_2} \frac{x^2}{2} + C_5x + C_6 \tag{37}$$

where

$$M_{0i} = \frac{4K_iI\hat{K}_i}{\pi R}, \quad K_i = \frac{\sigma_{0i}}{(\alpha_i\epsilon_{0i})^{1/n_i}}, \quad \hat{K}_i = \frac{\sqrt{\pi}}{2}\frac{\Gamma(1.0 + 0.5/n_i)}{\Gamma(1.5 + 0.5/n_i)} \tag{38}$$

in which

$$\Gamma(u) = \int_0^\infty \xi^{u-1}\exp(-\xi)d\xi \tag{39}$$

is the gamma function. Enforcing boundary and compatibility conditions, the constants C_1–C_6 are

$$C_1 = -\frac{1}{R}\left(\frac{M}{M_{01}}\right)^{n_1}\left[\frac{\hat{a}}{2}\left\{1-\left(\frac{t}{t_e}\right)^{n_1}\right\}+\frac{L_w}{2}\left(\frac{t}{t_e}\right)^{n_1}\right] + \frac{1}{R}\left(\frac{M}{M_{02}}\right)^{n_2}\frac{L_w}{2}\left(\frac{t}{t_e}\right)^{n_2}$$

$$C_2 = \frac{L}{R}\left(\frac{M}{M_{01}}\right)^{n_1}\left[-\frac{L}{8}+\frac{\hat{a}}{4}\left\{1-\left(\frac{t}{t_e}\right)^{n_1}\right\}+\frac{L_w}{4}\left(\frac{t}{t_e}\right)^{n_1}\right] - \frac{L}{R}\left(\frac{M}{M_{02}}\right)^{n_2}\frac{L_w}{4}\left(\frac{t}{t_e}\right)^{n_2}$$

$$C_3 = -\frac{1}{R}\left(\frac{M}{M_{01}}\right)^{n_1}\frac{L_w}{2}\left(\frac{t}{t_e}\right)^{n_1}+\frac{1}{R}\left(\frac{M}{M_{02}}\right)^{n_2}\frac{L_w}{2}\left(\frac{t}{t_e}\right)^{n_2}$$

$$C_4 = \frac{1}{R}\left(\frac{M}{M_{01}}\right)^{n_1}\left[-\frac{L^2}{8}+\frac{L\hat{a}}{4}\left\{1-\left(\frac{t}{t_e}\right)^{n_1}\right\}+\frac{LL_w}{4}\left(\frac{t}{t_e}\right)^{n_1}-\frac{\hat{a}^2}{8}\right] - \frac{1}{R}\left(\frac{M}{M_{02}}\right)^{n_2}\frac{LL_w}{4}\left(\frac{t}{t_e}\right)^{n_2}$$

$$C_5 = 0$$

$$C_6 = \frac{1}{R}\left(\frac{M}{M_{01}}\right)^{n_1}\left[-\frac{L^2}{8}+\frac{L\hat{a}}{4}\left\{1-\left(\frac{t}{t_e}\right)^{n_1}\right\} + \frac{L_w}{2}\left(\frac{L}{2}-\frac{L_w}{4}\right)\left(\frac{t}{t_e}\right)^{n_1}-\frac{\hat{a}^2}{8}\right] - \frac{1}{R}\left(\frac{M}{M_{02}}\right)^{n_2}\frac{L_w}{2}\left(\frac{t}{t_e}\right)^{n_2}\left[\frac{L_w}{4}-\frac{L}{2}\right] \quad (40)$$

APPENDIX C

The expression for the partial derivatives $\partial I_B/\partial\theta$ and $\partial L_B^d/\partial\theta$ are given as follows:

$$\frac{\partial I_B}{\partial\theta} = 4\theta F_B(\theta)^2 \quad (41)$$

$$\frac{\partial L_B^d}{\partial\theta} = \frac{1}{[A_3G_1(\theta)]^2}\{A_3G_1(\theta)[A_1G_{n_1}'(\theta)+A_2G_{n_2}'(\theta)] - A_3G_1'(\theta)[A_1G_{n_1}(\theta)+A_2G_{n_2}(\theta)]\} \quad (42)$$

in which

$$G_k(\theta) = \left(\cos\frac{\theta}{2}-\frac{1}{2}\sin\theta\right)^{-k}$$
$$G_k'(\theta) = \frac{k}{2}\left(\sin\frac{\theta}{2}+\cos\theta\right)G_{k+1}(\theta) \quad (43)$$

$$A_1 = \left(\frac{M}{M_{01}}\right)^{n_1}\left[\frac{\hat{a}}{2}-\frac{L_w}{2}\right]C^{-n_1}\frac{1}{\alpha_1\left(\frac{M}{M_1^*}\right)^{n_1-1}}$$

$$A_2 = \left(\frac{M}{M_{02}}\right)^{n_2}\left[\frac{L_w}{2}\right]C^{-n_2}\frac{1}{\alpha_1\left(\frac{M}{M_1^*}\right)^{n_1-1}}$$

$$A_3 = \left(\frac{M}{M_1^*}\right)\epsilon_{01}\left[\frac{\hat{a}}{2}-\frac{L_w}{2}\right]C^{-1}+\left(\frac{M}{M_2^*}\right)\epsilon_{02}\left[\frac{L_w}{2}\right]C^{-1} \quad (44)$$

where $C = 1$ or $C = 4/\pi$ according to whether 0 deg $\leq 2\theta \leq$ 90 deg or $2\theta \geq$ 120 deg, respectively. When 90 deg $\leq 2\theta \leq$ 120 deg, C can be interpolated from the foregoing two limits (Brust, 1987).